

Article

First-Principles Assessment of the Structure and Stability of 15 Intrinsic Point Defects in Zinc-Blende Indium Arsenide

Qing Peng ^{1,*}, Nanjun Chen ¹, Danhong Huang ², Eric R. Heller ³, David A. Cardimona ² and Fei Gao ^{1,*}

¹ Nuclear Engineering and Radiological Sciences, University of Michigan, Ann Arbor, MI 48109, USA; njchen@umich.edu

² Space Vehicles Directorate, Air Force Research Laboratory, Kirtland AFB, Albuquerque, NM 87117, USA; danhong.huang@us.af.mil (D.H.); david.cardimona@us.af.mil (D.A.C.)

³ Materials and Manufacturing Directorate, Air Force Research Laboratory, Wright Patterson AFB, OH 45433, USA; e-eric.heller@wpafb.af.mil

* Correspondence: qpeng.org@gmail.com (Q.P.); gaofei@umich.edu (F.G.)

Received: 4 December 2018; Accepted: 15 January 2019; Published: 17 January 2019



1. Defect Formation Energy in As-Rich Environment

The formation energy refers to the lowest formation energy among various charge states of $-4 \leq q \leq 4 + e$. Due to the influence of the chemical environment, the defect formation energy is a function of Fermi level E_F . The lowest formation energies as functions of E_F for each of fifteen defective configurations are presented in Figure S1 for As-rich environments.

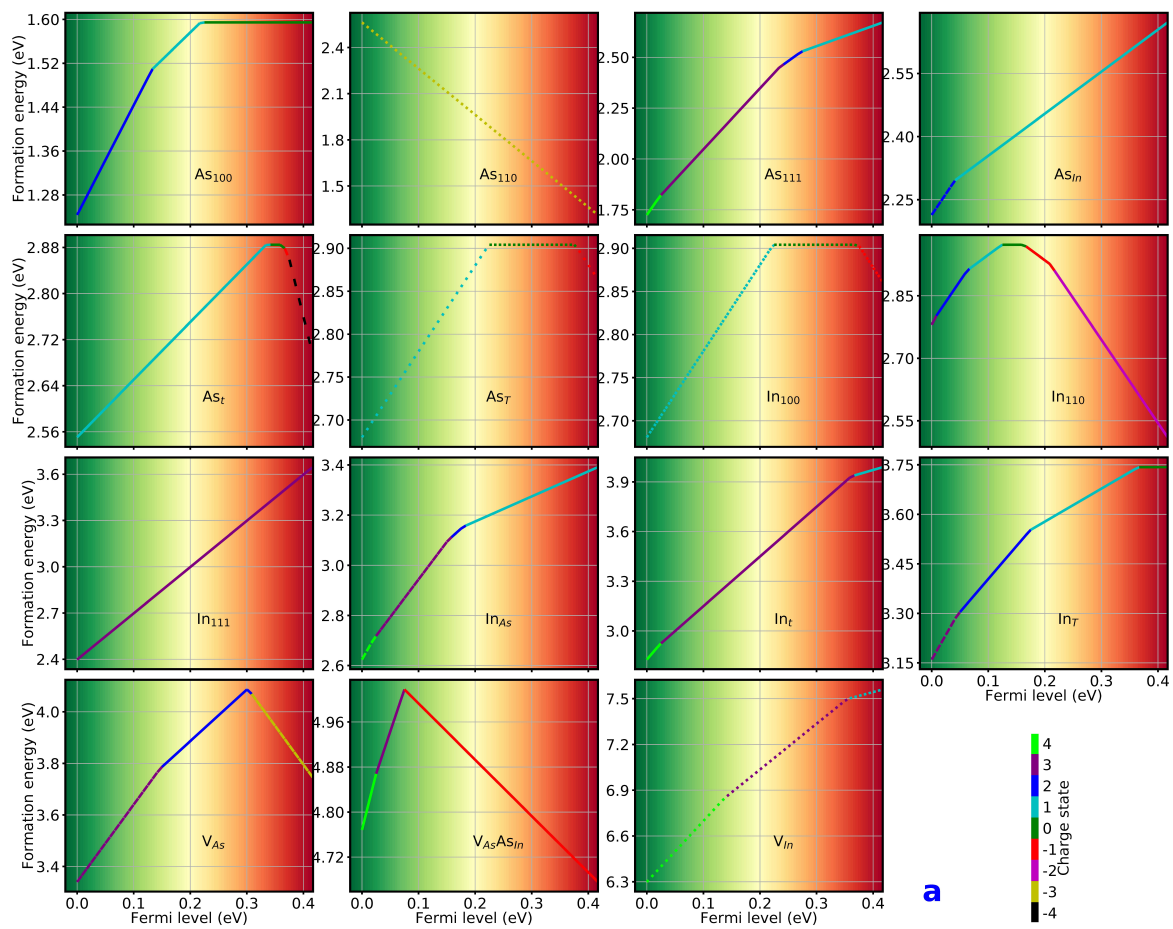


Figure S1. Formation energies as functions of E_F in the As-rich environments for fifteen different types of point defects in *zb*-InAs with all possible charge states from -4 to +4 marked by corresponding colors. The y-axis for each subplot is self-adapted for a better view. The different doping regimes near valance bands (*p*-type) and conduction bands (*n*-type) are displayed.

2. Defect Formation Energy in In-Rich Environment

The lowest formation energies as functions of E_F for each of fifteen defective configurations are presented in Figure S2 for In-rich environments.

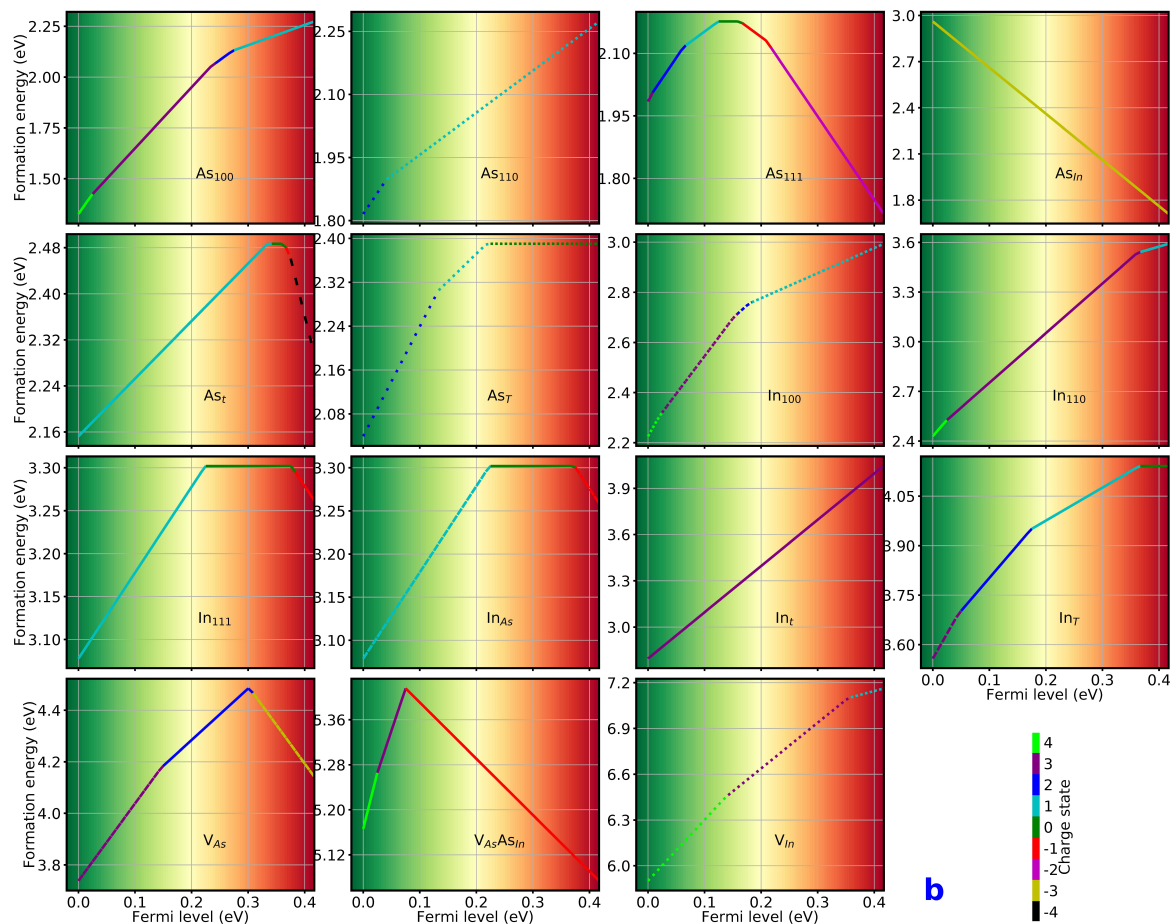


Figure S2. Formation energies as functions of E_F in the In-rich environments for fifteen different types of point defects in *zb*-InAs with all possible charge states from -4 to +4 marked by corresponding colors. The y-axis for each subplot is self-adapted for a better view. The different doping regimes near valance bands (*p*-type) and conduction bands (*n*-type) are displayed.



© 2019 by the authors. Licensee MDPI, Basel, Switzerland. This article is an open access article distributed under the terms and conditions of the Creative Commons Attribution (CC BY) license (<http://creativecommons.org/licenses/by/4.0/>).